Integrated Interpretation of Magnetic and ERT Data to Characterize a Landfill in the North-West of Cologne, Germany

Ismael M. Ibraheem,[1] Bülent Tezkan,[1] and Rainer Bergers[1]

Abstract—Electrical resistivity tomography (ERT) and ground magnetic surveys were applied to characterize an old uncontrolled landfill in a former exploited sand and gravel quarry in an area to the north-west of the city of Cologne, Germany. The total magnetic field and its vertical gradient were recorded using a proton precession magnetometer to cover an area of about 43,250 m^2. The magnetic data were transferred to the frequency domain and then reduced to the north magnetic pole. The amplitude of the analytical signal was calculated to define the magnetic materials within and outside the landfill. Eight ERT profiles were constructed based on the results of the magnetic survey using different electrode arrays (Wenner, dipole–dipole, and Schlumberger). In order to increase both data coverage and sensitivity and to decrease uncertainty, a non-conventional mixed array was used. The subsurface resistivity distributions were imaged using the robust (L1-norm) inversion method. The resultant inverted subsurface true resistivity data were presented in the form of 2D cross sections and 3D fence diagram. These non-invasive geophysical tools helped us to portray the covering soil, the spatial limits of the landfill, and the depth of the waste body. We also successfully detected low resistivity zones at deeper depths than expected, which probably be associated with migration pathways of the leachate plumes. The findings of the present study provide valuable information for decision makers with regards to environmental monitoring and assessment.

Keywords: Landfill, leachate plume, magnetic gradiometry, electrical resistivity tomography (ERT), mixed array.

1. Introduction

Geophysics has been successfully applied to investigate dumpsites and has become a very important tool in this regard. The greatest advantage of using geophysical methods is that they are environmentally benign where they cause no disturbance of subsurface structures and materials (Reynolds,

2011). Several geophysical techniques improved their power in detection the geometry of waste deposits in a faster, cheaper, and non-destructive way. Among these techniques are magnetic methods (Marchetti et al., 2002; Prezzi et al., 2005), electrical resistivity and electromagnetic prospecting (Baawain et al., 2018; Bernstone & Dahlin, 1997; Candansayar & Tezkan, 2006; De Carlo et al., 2013; Frangos, 1997; Helene et al., 2020; Karlik & Kaya, 2001; Martinho & Almeida, 2006; Morita et al., 2020; Saraev et al., 2020; Tezkan et al., 2000), ground penetration radar (GPR) (Orlando & Marchesi, 2001; Porsani et al., 2004; Wu & Huang, 2006), seismic methods (Carpenter et al. 1991; De Laco et al., 2003; Missiaen & Feller, 2008) in addition to the use of a combination of more than one geophysical method (Appiah et al., 2018; Genelle et al., 2014; Tezkan et al., 1996; Yannah et al., 2019). Moreover, investigating leachates and locating possible paths of pollution plumes in landfill areas using near-surface geophysical techniques have been studied by several scientists (e.g. Mepaiyeda et al., 2019; Ogilvy et al., 2002; Ramalho et al., 2013; Song et al., 2019).

Landfills are the most common places for the elimination and storage of huge amounts of domestic and industrial wastes of heterogeneous properties. They represent one of the most critical and serious environmental problems all around the world, but especially in developing countries. Despite the fact that current restricted national regulations prohibit non-controlled landfills, a tremendous number of old landfills have been found in Germany. To remediate this problem, the determination of the vertical and horizontal distributions of buried waste is essential. In many illegal landfills, household refuse, metallic objects, building debris, and dangerous industrial

[1] Institute of Geophysics and Meteorology, University of Cologne, Pohligstrsse 3, 50969 Cologne, Germany. E-mail: ismael.ibraheem@geo.uni-koeln.de; ismail.geo@gmail.com

wastes were often dumped in small gravel pits in an uncontrolled manner. This usually happens without knowledge or in a poorly documented way and without any landmarks at the surface (Tezkan, 1999). Unfortunately, most closed old landfills are unlined, causing a migration of contaminant plumes off-site. This leads to a serious risk for the environment and can be a major source of groundwater contamination, which presents a real threat to human beings, animals and plants. This in turn makes the remediation efforts problematic. Generally, shallow boreholes are used for the observation, monitoring, and evaluation of old waste sites. These are, however, very costly and run a considerable risk of damaging the liners of the landfill, thus causing a downward migration of contaminants.

Geophysical techniques can assist in the monitoring of landfills and provide a rapid, noninvasive means of characterizing the distribution of buried waste materials within them. Despite the difficulties in carrying out geophysical surveys in many areas where deposit sites are situated, they are definitely much cheaper compared to observation boreholes. Difficulties usually occur due to the presence of obstacles such as vegetation and cultural noise in addition to the complexity of the interpretation caused by inhomogeneity within the waste site. Although it is difficult to get detailed information about the dumpsite's contents, a geophysical exploration is essential for estimating the risk level posed by contamination plumes.

The present research focuses on the integrated interpretation of magnetic and ERT methods in order to detect the geometry of a landfill located to the north-west of Cologne and to determine any possible contamination plumes. These methods constitute efficient tools in differentiating the cover soil, natural host soil and the waste body inside the landfills. Magnetic methods play a major role in defining places with high magnetic anomalies likely connected with buried ferrous objects within the site. Moreover, the vertical gradient of the magnetic field is more sensitive to small magnetic objects that have a high magnetization compared to their surrounding (Kirsch, 2009; Soupios & Ntarlagiannis, 2017). Because landfills have a relatively higher conductivity than the surrounding host, this makes the electrical resistivity

tomography technique highly suitable for their detection (Simyrdanis et al., 2018; Yannah et al., 2019).

2. Background of the Waste Site

The investigated area is an old landfill situated in the north-west of Cologne, Germany (Fig. 1). It was formed as the result of long-term dumping of various wastes. It was exploited as a sand and gravel pit from the 1940s to the 1950s; then—gradually—the empty part of the ground was filled with different kinds of wastes including household refuse, construction waste, industrial waste, cinder, tires, wood, plastic, military fences, etc. from the mid-1950s. The site was closed and covered with an irregular thin soil layer in the 1980s. The site has a flat topography at its southern and central parts and relatively low topography at the northern part. The investigated area was recently covered with grass. Because this is an old site, it is difficult to know its exact distribution and the nature of the materials within it. Thanks to information from shallow exploratory boreholes (Fig. 1), the maximum depth to the base of the waste is expected to be up to 8 m (Table 1). The boreholes show that the landfill has shallow depths at its southern part which increase towards the center and the northern parts. The maximum depths are recorded at boreholes B3 (7.8 m) at the center and B11 (7.9 m) at the north-eastern corner of the landfill.

The geological information for the area in which the waste site is situated was inferred from a geological cross section (Fig. 2) passing about 1 km to the west of the site. The topmost is a Pleistocene/Holocene floodplain fines layer with a thickness of 2–3 m overlying a Pleistocene gravelly sand layer which has a depth of approximately 18–25 m. The base of the sequence are Tertiary deposits. These deposits are composed of clay, brown coal and sand. The groundwater table has an average depth of 10 m (Heuser & Thielmann, 1986) and the groundwater flow direction is from the southwest to the north–east.

Moreover, according to the information obtained from Well W2 (see Fig. 1) which reaches a depth of 27 m, the subsurface lithology consists mainly of successive layers of sand and gravel. Waste materials
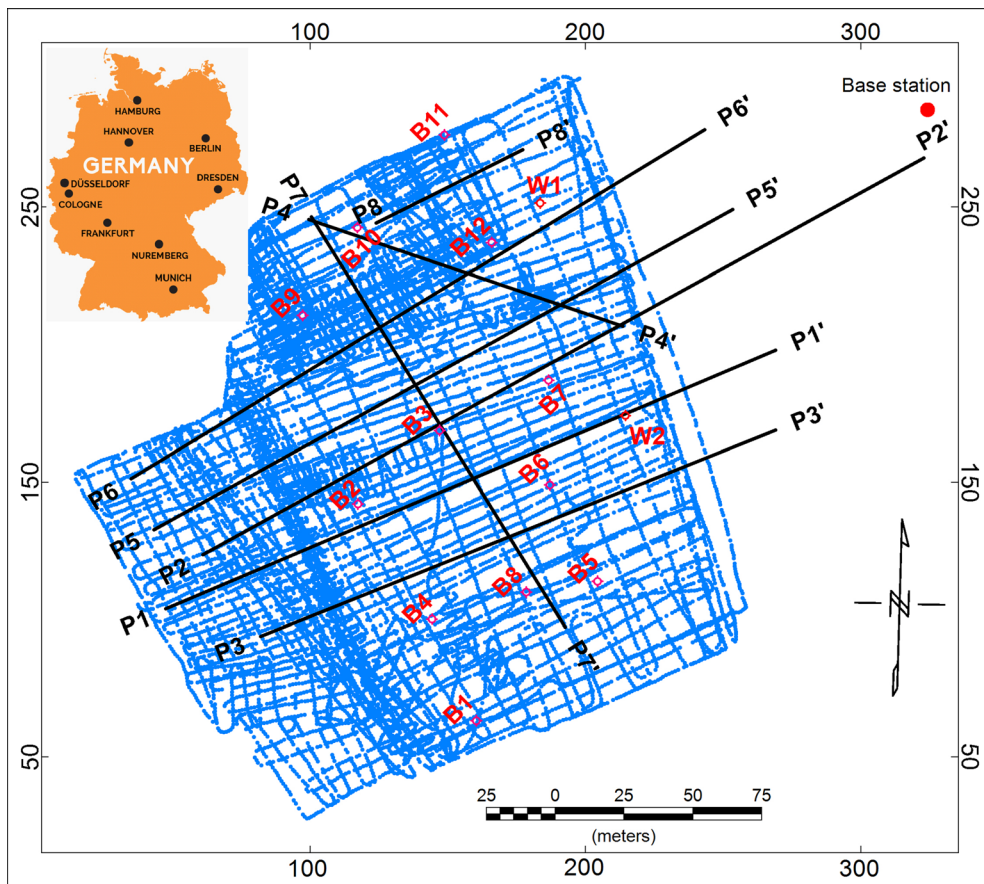
Figure 1
Map of the investigated waste site, north-west of Cologne, Germany, showing magnetic stations and ERT profiles. Blue points represent the locations of the magnetic stations. ERT profiles are represented by black lines. The red point refers to the location of the magnetic base station. Locations of two observation wells (W1 and W2) and 12 exploratory shallow boreholes (B1–B12) are also presented

Table 1

Depths of shallow control boreholes to the base of the landfill

Borehole	B1	B2	B3	B4	B5	B6	B7	B8	B9	B10	B11	B12
Depth (m)	0.1	1.8	7.8	1.3	0.5	3.9	3.2	3.2	4.5	6.4	7.9	3.5

(rubble and debris) occupy the first 1.5 m. Sequences of sand and gravel up to depth of 16 m have been encountered. A thin clay layer with a thickness of 0.5 m is determined at depth of 10 m. This follows by a 10 m-layer of gravel representing the Pliocene sediments underlined by a Tertiary fine sand layer. The groundwater level ranges between 9.5 and 10.5 m

which is in agreement with the information obtained from the geological cross section (Fig. 2).

Nowadays, the area of the landfill is partly visible as a local depression, presumably caused by shrinking processes of the dumped materials over the years. This low topography compared to its surroundings is expected to cause accumulation of rainwater leading
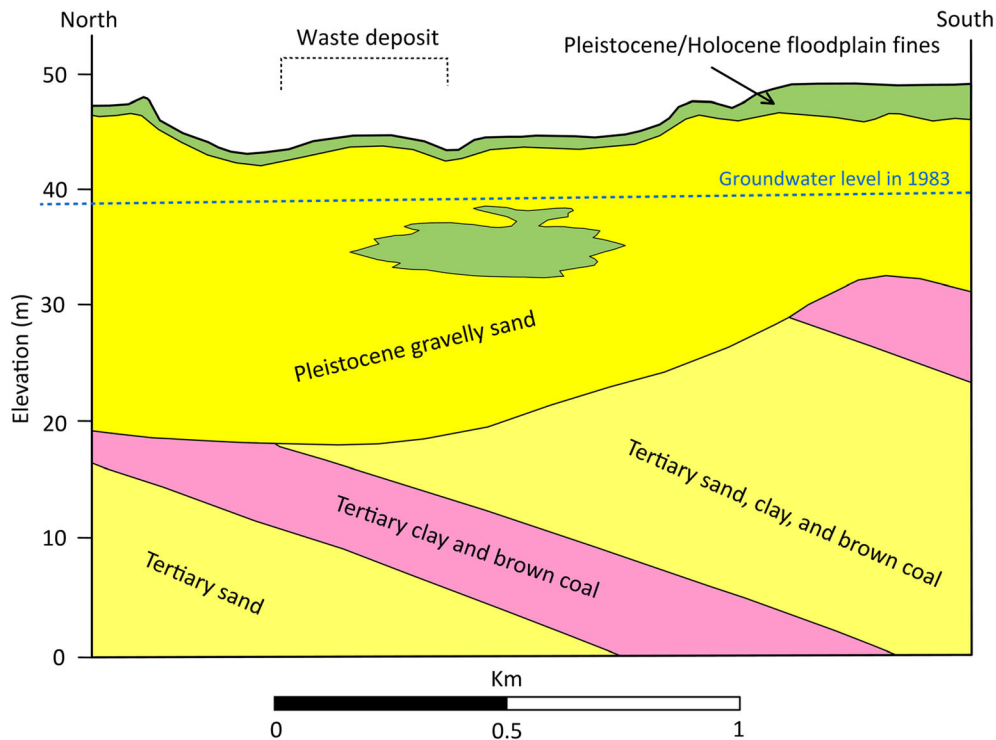
Figure 2
Geological cross section passing close to the waste deposit site (Heuser & Thielmann, 1986)

to increase infiltration through the waste materials into deeper horizons. This is likely to contribute to the generation of leachate and thus to increase the environmental impact. Thinkable remedy measures could be levelling the area up, above the surroundings and/or installing a barrier to steer the percolation of rainfall through the neighboring undisturbed soils instead of the landfill.

3. Materials and Methods

The study made use of two geophysical techniques, namely magnetic and ERT. A combination of these two methods can help to reduce uncertainties in interpretation arising when only one method is used. The magnetic technique has been used in several environmental applications to map magnetic materials within waste sites (Appiah et al., 2018; Dumont et al., 2017; Wemegah et al., 2017). Moreover, the ERT method is considered very suitable for solving

environmental problems due to the conductive nature of contaminants. In the present study, the results of the magnetic survey served as a base for setting up the locations of ERT profiles.

3.1. Magnetic Survey

The magnetic method has proven its effectivity for solving environmental problems and is considered as one of the most rapid, efficient, and powerful methods for detecting the lateral extents of landfills which—in most cases—contain erratically distributed highly-magnetized materials (Appiah et al., 2018). Moreover, the magnetic gradiometry as a near-surface geophysical method is very effective in determining such relatively small magnetic bodies within the upper few meters of the ground. These highly magnetic objects produce distinct positive anomalies when plotted in the form of magnetic maps.

Two Gem-System GSM-19 T Proton Magnetometers (sensitivity < 0.1 nT, resolution 0.01 nT, and absolute accuracy 1 nT) were used to carry out the magnetic survey. One was used as a base station located outside the landfill to observe continuously temporal variations of the magnetic field, and the other was used as a roving magnetometer to collect the magnetic data over the investigated area (Fig. 3a). Both instruments were automatically synchronized to

UTC (Universal Time Coordinate), and the GPS timing controls their cycling in order to perform the diurnal corrections later. The total magnetic field intensity at two sensors at heights of 0.8 m and 1.8 m from the ground surface were captured, and consequently the resulting vertical gradient was obtained. Magnetic data were acquired in three phases during the period between November 2018 and January 2019, by taking continuous measurements (walking
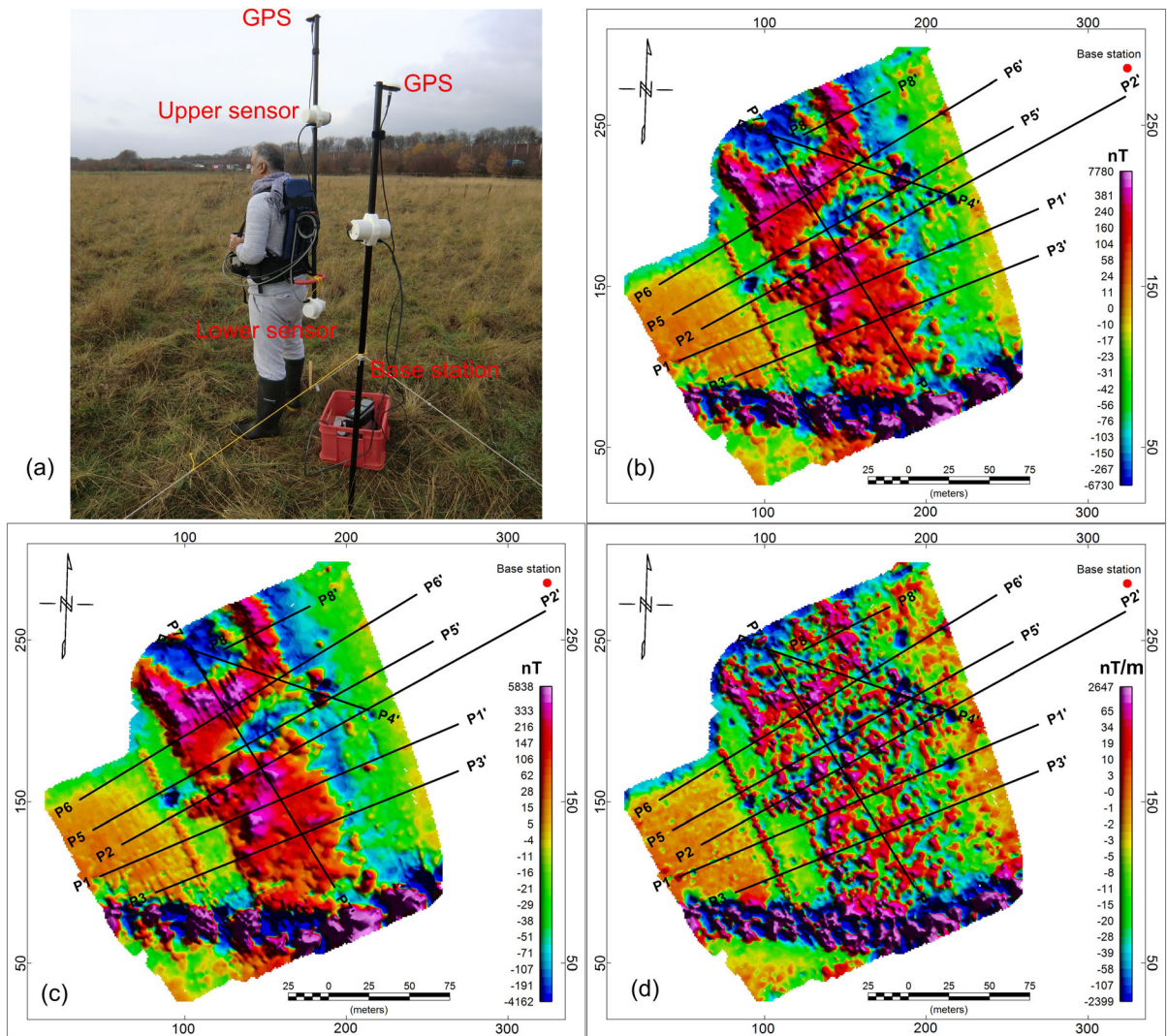

Figure 3

a A photo shows the base station and the roving magnetometer with GPS and two sensors in gradiometer configuration mounted on a back pack, **b** magnetic anomaly map measured by lower sensor at 0.8 m height from ground surface, **c** magnetic anomaly map measured by upper sensor at 1.8 m height from ground surface, and **d** vertical gradient magnetic map. The boundaries of the landfill can be obviously distinguished from the undisturbed regions. A linear magnetic anomaly with high magnetic values at the southern portion of the maps is produced by buried gas pipelines. Black lines represent the locations of ERT profiles

gradiometer mode) with a sampling frequency of one station per 0.5 s (Fig. 1). The measurements were extended into the undisturbed area outside the potential dumping site. The daily magnetic variations in the earth's magnetic field were eliminated from the data obtained by a single sensor by subtracting the field value at the base station from that at the roving survey station.

It is worth noting that gradiometry magnetic measurements automatically eliminate temporal magnetic variations and regional background fields, which is one of the significant advantages of this technique (Hinze et al., 2013; Sharma, 1997). The acquired magnetic data were gridded using the minimum curvature technique; then magnetic maps were generated to show the distribution of magnetic materials within the landfill. As a result, three magnetic maps representing the total magnetic field at the lower and upper probes in addition to the vertical gradient of the magnetic field were obtained (Fig. 3). The ranges of the recorded values are – 6730 to 7780 nT, − 4162 to 5838 nT, and − 2399 to 2647 nT/m for the magnetic data obtained from the lower sensor, the upper sensor and vertical gradient, respectively. The comparison between the magnetic anomaly maps obtained by a single sensor (Fig. 3b and c) and the vertical gradient (Fig. 3d) shows the advantage of the latter because it has better information content and a higher resolution of near-surface magnetization variations (Reynolds, 2011). The magnetic maps obtained by the lower and upper sensors (Fig. 3b–d) show the landfill as a distinct highly magnetic zone separated from its surroundings, which helps in delineating its borders. The general boundaries of the landfill are clearly depicted using the three previously mentioned magnetic maps.

The magnetic data were transferred to the frequency domain using Fast Fourier Transform (FFT). Subsequently, a reduction to the pole (RTP) filter was applied to the magnetic data—assuming only induced magnetization—to improve the visual interpretation of the magnetic anomalies by disposing of the distortion caused by the inclination of the earth's magnetic field and by shifting the magnetic anomalies to be over their sources (Ibraheem et al., 2018a, b, 2019) using values of 66.3° and 2° for inclination and declination of the survey area,

respectively. Magnetic anomalies are usually generated from either an induced magnetization or a permanent magnetization. Generally, iron objects exhibit both induced and permanent magnetizations. In the case of the present study, we expect that remanent magnetization plays a significant role in the magnetic properties of the magnetic materials within a landfill. In two dimensions, the analytical signal is independent from the magnetization direction but in three dimensions it is dependent of several factors including depth, extent and plunging of the magnetic source as well as the directions of both the body's magnetization and the Earth's magnetic field. However, the AS amplitude may complement the RTP magnetic map for qualitatively edge detection purposes especially when the magnetic sources are located at shallow depths (Li, 2006) which is the case in our study. The amplitude of the analytical signal (AS) for 3D structures is given by the following equation (Roest et al., 1992):

$$AS(xy) = \sqrt{\left(\frac{\partial M}{\partial x}\right)^2 + \left(\frac{\partial M}{\partial y}\right)^2 + \left(\frac{\partial M}{\partial z}\right)^2}$$

where M is the measured magnetic field at (x, y), and $\frac{\partial M}{\partial x}$, $\frac{\partial M}{\partial y}$ and $\frac{\partial M}{\partial z}$ are the derivatives of the measured field in x, y, and z directions, respectively. The amplitude of the AS produces bell-shaped anomalies over magnetic sources. Therefore, its maxima are very powerful in determining the edges of magnetic bodies (Arisoy & Dikmen, 2013; Isles & Rankin, 2013; Jeng et al., 2003).

3.2. Electrical Resistivity Tomography (ERT) Survey

ERT is the most commonly used electrical technique: measurements of ground resistivity are made by injecting an electric current into the subsurface via two current electrodes. Then the difference in the electrical potential is measured as a voltage using two additional potential electrodes. The obtained voltages will be converted into apparent resistivity values. The set of electrodes is shifted each time by one electrode separation laterally until the entire array is scanned. Then, the electrode spacing is increased incrementally by one electrode. This process is repeated until the appropriate number of levels

has been covered. As a result, a pseudo-section is plotted. The acquisition procedure is a software-controlled process. These apparent resistivities are used to model the true resistivity distribution of the subsurface (Reynolds, 2011; Telford et al., 1990). The resolution of the ERT survey is mainly based on the type of electrode configuration, the spacing between electrodes, the signal-to-noise (S/N) ratio, and the type of inversion algorithm (Cardarelli & De Donno, 2019).

The increase in the concentration of free ions caused by the presence of contaminated materials within a landfill leads—in comparison to the host medium—to a decrease of the resistivity of the waste body. This in turn enables the determination and mapping of contaminated soils in dumping sites. Therefore, the ERT method plays a major role in detecting the wastes and their contaminant plumes due to the high contrast of resistivity between the contaminating waste body and the natural environment (Appiah et al., 2018; Baawain et al., 2018; Helene et al., 2020). The choice of the suitable electrode configuration depends on the structure to be investigated, the noise level, and the sensitivity of the resistivity meter. Commonly used data acquisition configurations include Wenner, dipole–dipole, Schlumberger, among others. The Wenner array is considered a very suitable choice in areas with a high background noise as it has a strong signal strength (good S/N ration) and is sensitive to vertical changes and less sensitive to lateral variations in the subsurface's resistivity. Therefore, it is very powerful in resolving vertical resistivity changes (horizontal structures). On the other hand, the dipole–dipole array has good data coverage as well as good sensitivity to horizontal changes in the subsurface's resistivity, but usually it suffers from background noise and has a lower S/N ratio than the Wenner array. It is therfore very suitable for mapping vertical structures. The Schlumberger array is moderately sensitive to horizontal and vertical structures. It has a stronger signal strength than dipole–dipole array but a weaker one than the Wenner array (Loke, 2020). More information about the properties of different arrays can be found in Dahlin and Zhou (2004) and Zhou and Dahlin (2003). In landfills, one can expect high horizontal and vertical variations in the subsurface's resistivity. Therefore, combining measurements of different electrode configurations to obtain good properties from several arrays and thus getting useful results, which cannot be obtained by using only one individual array is quite advantageous (Kaufmann & Quinif, 2001; Zhou et al., 2002). In this research, the resistivity data obtained by different arrays (Wenner, dipole–dipole, and Schlumberger) were merged in one dataset (mixed array) to form a non-conventional array format (Loke, 2020). In comparison to other electrode configurations, a mixed array has a better subsurface data coverage, reduced uncertainty, higher sensitivity and a good lateral and vertical resolution (Zhou et al., 2002).

As it would be time consuming to carry out ERT measurements over the entire dumpsite, the layout of preselected ERT profiles was planned to cut the most interesting anomalies obtained from the magnetic results and to cover most of the area of the landfill and its surroundings. Eight ERT profiles were measured using ABEM Terrameter LS. In each measurement, 64 electrodes and 4 cables were used. The electrode spacing varies from 0.75 to 3 m in the second and third cable and from 1.5 to 6 m in the first and fourth cable along the measured profile as shown in Table 2. The roll-along procedure was used to extend the area covered by the 2D survey. The standard Wenner and dipole–dipole configurations were used to carry out the ERT survey. The Schlumberger array was also used in profile P5. The contact resistances of electrodes (contact impedance) measured before the data acquisition were less than 2.5 kΩ, which is low enough to obtain good data. In case of high contact impedance values, a little amount of water was used to reduce the value of the contact impedance and to improve the contact with the soil. All bad data points, negative apparent resistivity values, and data values with high variation coefficients were removed manually from the datasets. The apparent resistivity data obtained from different arrays were combined in one dataset for each profile to form what is called a mixed array. This was carried out for all profiles during the processing of the ERT data.

The obtained ERT data were processed with the aid of Res2DInv software by Geotomo (Loke, 2020). The apparent resistivity data were inverted into

subsurface 2D resistivity models using the L1-norm regularization inversion technique (called also robust or blocky method) which minimizes the absolute differences between measured and calculated apparent resistivity values by an iterative process (Loke et al., 2003; Wolke & Schwetlick, 1988), in which the accuracy of the data fit is expressed in terms of the absolute error (Claerbout & Muir, 1973). The topography was incorporated into the inversion model to eliminate any artificial anomalies generated by the effect of the topography. The mathematical formulations used by the L1-norm and L2-norm optimization techniques have been discussed in the geophysical literature (e.g. Cardarelli & De Donno, 2019; Leucci, 2020; Loke, 2020; Loke et al., 2003).

4. Results and Discussion

A combination of more than one geophysical method is commonly applied in near-surface studies to reduce the ambiguity problem related to the interpretation of the data. The spatial mapping provided by the magnetic survey helps to detect the most interesting places for the follow-up ERT survey. Compared with the magnetic maps, the RTP magnetic maps (Fig. 4) reflect a northward shift in the locations of the magnetic anomalies (Fig. 3). Moreover, the RTP magnetic maps clearly demonstrate that the area is characterized by several distinguishable magnetic zones denoted Z1, Z2, Z3, and Z4, which reflect different kinds of wastes. Zones Z1 and Z3 show negative low magnetic values, which can be interpreted as non-magnetic materials such as plastic, rubber, glass…etc. On the other hand, zones Z2 and Z4 show highly magnetic anomalies which can be associated with magnetic materials such as drums, construction materials, industrial wastes, military fences…etc. A linear magnetic anomaly can be seen in the southern part of the map, reflecting a large magnetic source which is interpreted as gas pipelines. Another linear magnetic anomaly trending SE-NW to the west of the landfill can be interpreted as a buried old road. Moreover, several magnetic anomalies are distributed outside the landfill, some of them (anomalies A1 and A2) are associated with known metallic bodies (two metal tubes elevated about 1 m

over the ground surface within the observation boreholes) and, in addition, a metallic sign (anomaly B3). The AS maps (Fig. 5) reflect a clear and detailed image of the magnetic anomalies associated with buried magnetic sources of different sizes and depths within the dumpsite. Moreover, the boundaries of the landfill are clearly distinguished compared to other magnetic maps. High amplitude anomalies (A1, A2, and A3) have been interpreted as culture noise because they are produced by metallic bodies seen on the surface. Local highly magnetic anomalies can be noticed within the undisturbed geology outside the landfill particularly in the eastern part referring to metallic objects in the subsurface or possibly unexploded ordinances (UXO) from the Second World War (refer to Fig. 5c).

To investigate the geological formations of the subsurface, profile P2 (Fig. 5) was constructed as a long reference profile passing from the middle of the waste site with a length of 300 m and an electrode interval of 3 m. The L1-norm (blocky) technique was elected to perform the inversion process because it produces a sharper contrast between the resistivity values of the waste body and the host medium than the smoothness-constrained least-squares (L2-norm) inversion, and also because it is less sensitive to bad data points compared to L2-norm method (Dahlin & Zhou, 2004; Loke et al., 2003). However, the smoothness-constrained least-squares method, which minimizes the square of the differences between the measured and calculated apparent resistivities, usually produces smoothly distributed resistivities of the subsurface. Therefore, the interfaces between the subsurface layers cannot be precisely determined. The cell-based model used for 2D resistivity inversion, the inverted resistivity cross sections of profile P2, and the discrepancies between the 2D inversion results of the two inversion methods are shown in Fig. 6. The L1-norm inversion method produced models with sharper edges and, generally, better imaging results than the L2-norm. Moreover, the overall 2D resistivity image obtained by the robust inversion technique is consistent with the available geological information (refer to Fig. 3). The Pleistocene/Holocene floodplain fines layer has a thickness of 1–5 m whereas the depth to the base of the Pleistocene gravelly sand layer ranges from 16 to
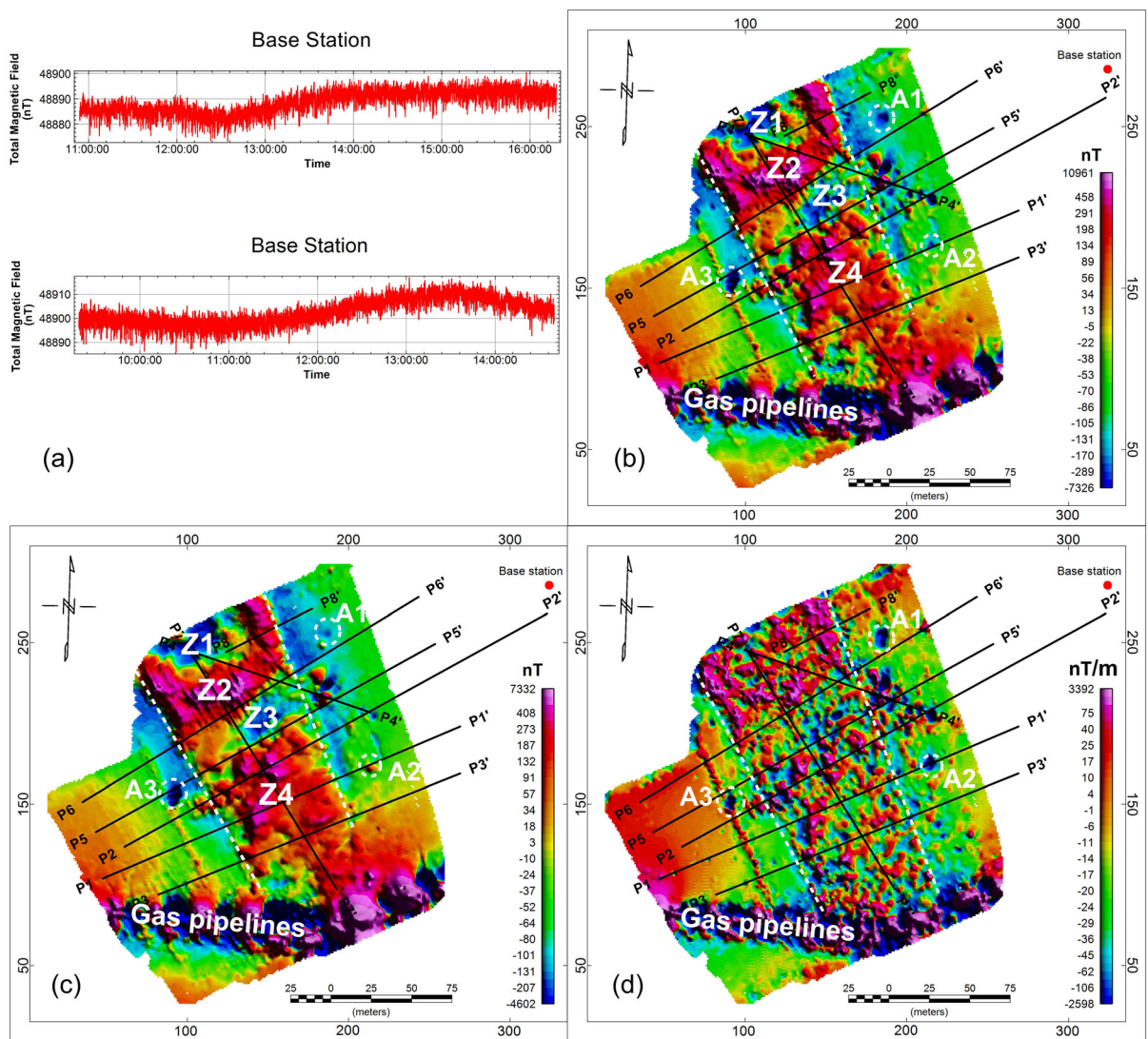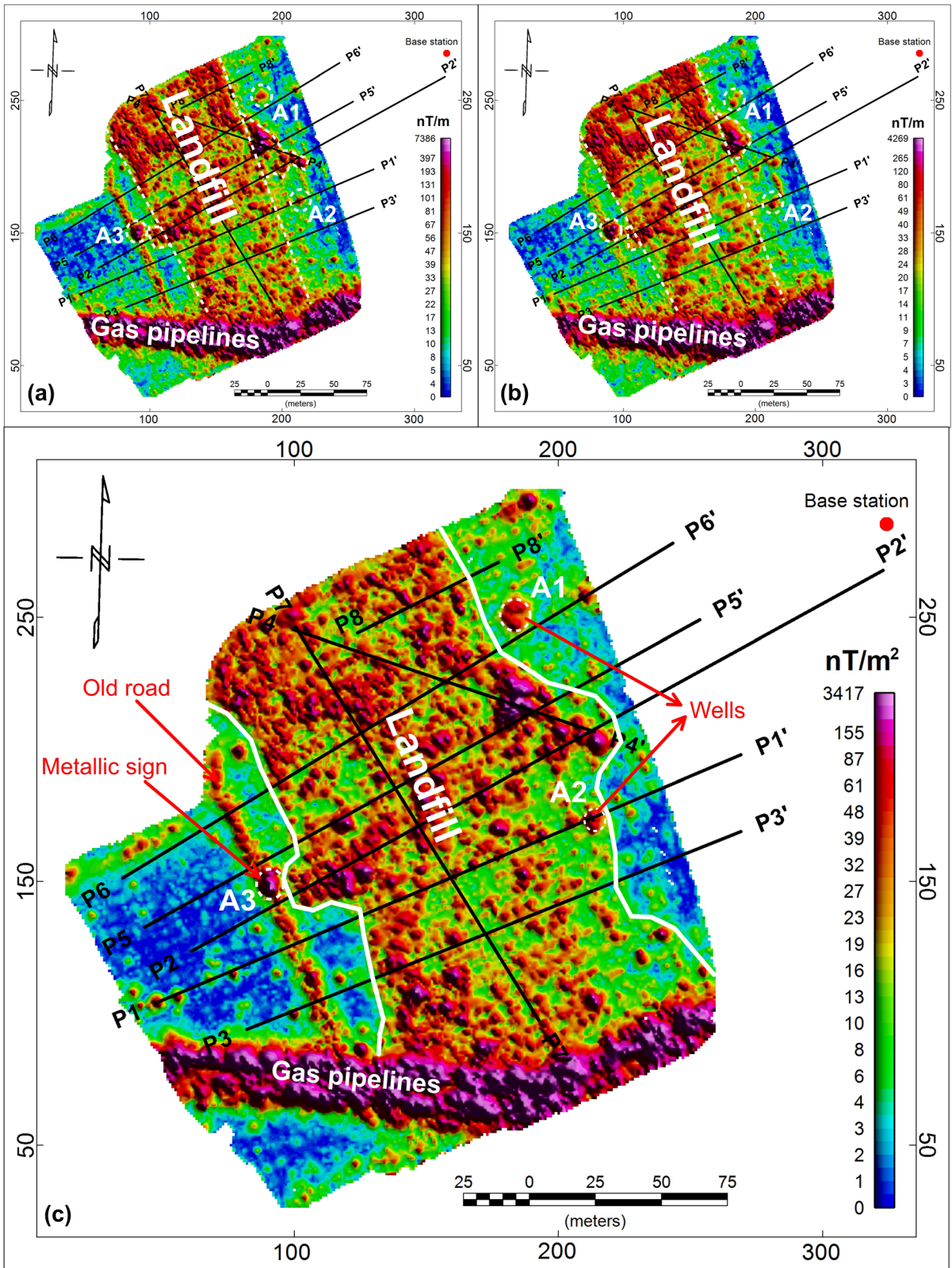
Figure 4

a Measurement of the total magnetic field intensity at the base station during 2 days of the magnetic survey for further corrections of diurnal variations, **b** RTP magnetic anomaly map measured by lower sensor at 0.8 m height from ground surface, **c** RTP magnetic anomaly map measured by upper sensor at 1.8 m height from ground surface, and **d** RTP vertical gradient magnetic map. The boundaries of the landfill (dashed white lines) can be obviously distinguished from the undisturbed regions. Very highly magnetic linear anomaly at the southern portion of the maps due to buried gas pipelines can be seen. Locations of ERT profiles are represented by black lines. Two magnetic anomalies (A1 and A2) produced by short metallic tubes (about 2 m length) inside the observation wells in addition to a magnetic anomaly (A3) generated by a metallic sign are also presented

28 m. The Tertiary deposits were also detected by the ERT survey. The results show that a very thin soil layer up to 2 m covers the wastes there where the depth to the base of the waste deposit reaches up to 13.5 m. The landfill starts from a distance of 50 m to a distance of 143 m where it is interrupted, and then it continues again as a thin layer to a distance of 185 m. The edges of the landfill obtained by the ERT survey along profile P2 are in agreement with the results of the magnetic survey. Borehole B2 confirms these ERT results. Moreover, the ERT results gives depths to the base of the landfill much greater than the

◄Figure 5
Analytical signal maps of **a** magnetic data of lower sensor, **b** magnetic data of upper sensor, and **c** vertical gradient data. Boundaries of the landfill are drawn with white lines. Magnetic anomalies (A1, A2, and A3) generated by known cultural noise are presented

depths obtained from boreholes B3 and B7 indicating a possible migration of the contaminants downwards to levels below the groundwater table. Furthermore, low resistivity values seen under the eastern border of the landfill between the distances 120 m and 142.5 m can be interpreted also as a possible contaminant plume.

Because each array has its distinctive advantages and disadvantages with regards to sensitivity to lateral and/or vertical variations, investigation depth, and quality of signal strength, the mixed array was selected to obtain a better representation of the subsurface in the landfill by combining the apparent resistivity data from the different used arrays into one dataset. Hence, better and more realistic subsurface 2D resistivity images can be obtained by pooling the advantageous properties of the arrays. Figure 7 shows the 2D ERT result of profile P4 using Wenner, dipole–dipole, and mixed arrays. This profile extends up to 120 m, and a roll-along procedure was used with 71 electrodes and an electrode spacing of 1.5 m. We merged 394 datum points and 14 data levels for the Wenner array and 1309 datum points and 46 data levels for the dipole–dipole array to obtain a mixed array with a larger dataset of 1595 datum points and 50 data levels. More information about the ERT profiles regarding the types of electrode arrays, number of electrodes, lengths of profiles, electrode spacing, number of datum points, data levels, layers, iterations, and absolute errors are found in Table 2. In comparison with the inverted resistivity models from the Wenner and dipole–dipole arrays, the model obtained from the mixed array provided much more detailed information about the subsurface, particularly in the area of the landfill. The depth to the base of the landfill is about 10 m, which exceeds the actual depth (6.4 m) obtained from the borehole B10 referring to a possible infiltration of the contaminants towards deeper layers. The resistivity values of this geoelectric cross section range between 1.44 and 1375 Ω m. Low resistivity values at depths up to 10 m on the resistivity model indicated the waste body. The cover soil layer has moderate to high resistivity values with a thickness of up to 2 m. The very high resistivity values along the ERT profile represent the gravelly sand layer. Furthermore, a remarkable low resistivity zone (about 10–15 Ω m) between the distances 50 m and 61 m and an intermediate resistivity zone (50–75 Ω m) between the distances 75 m and 85 m which are sandwiched by the gravelly sand layer can be interpreted as a possible leakage of contaminant in a downward direction. This could pose great threat to groundwater in the area of the dumping site.

The ERT profile P5 was measured using the Wenner, dipole–dipole, and Schlumberger arrays with 64 electrodes, and it was extended to a length of 240 m. As in the other ERT profiles, the data from the mentioned arrays were gathered in one dataset to increase the subsurface data coverage and to provide a good lateral and vertical resolution. Datum points of 345, 1059, and 745 and data levels of 14, 43, and 25 from Wenner, dipole–dipole, and Schlumberger respectively were merged to form a dataset of a mixed array with 1963 datum points and 71 data levels. Though the resistivity data were collected along the same profile, obvious discrepancies between the inverted 2D resistivity models from the Wenner, dipole–dipole, Schlumberger and mixed arrays are observed (Fig. 8). Some similarity between the Wenner array and the Schlumberger arrays and between the dipole–dipole array and mixed arrays can be noticed. Compared with the available geological information, the subsurface 2D resistivity model obtained from the mixed array is the more realistic one. Obvious contaminant plumes were detected at both edges of the landfill between the distances 78 m and 90 m and between the distances 147 m and 165 m. According to the borehole information, the waste body is at depths of up to 8 m, but the ERT results along this profile demonstrate that the leachate migrates from the landfill downwards and reaches a depth of 17.5 m.

Figure 9 shows the inverted 2D resistivity models from profiles P1, P3, and P6 which cross the dumpsite in lines parallel to the groundwater flow direction. The 2D resistivity models distinctly show a low
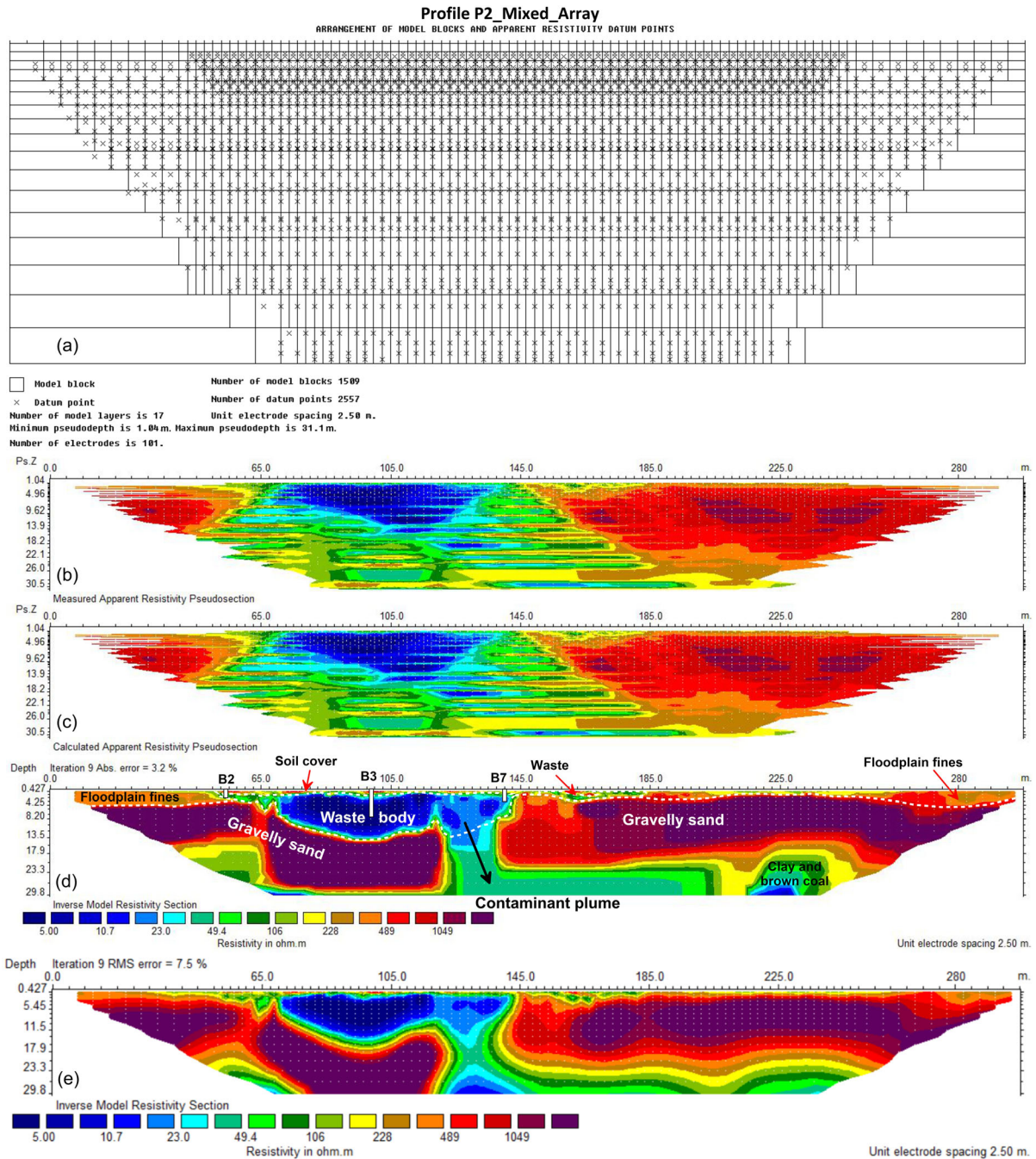
Figure 6

a The cell-based model used for 2D resistivity inversion of ERT profile P2. **b** Measured and **c** calculated apparent resistivity pseudosections of profile P2 using non-conventional mixed array. **d** The inverted resistivity 2D model using robust inversion (L1-norm) of the ERT data after 9 iterations (absolute error = 3.2%). **e** The inverted resistivity 2D model using the smoothness-constrained least-squares (L2-norm) inversion of the ERT data after 7 iterations (RMS error = 7.6%). Depths to the base of the landfill obtained from boreholes B2 located 11 m to south of profile P2 and B7 located 5 m to the south of profile P2 have been drawn on the 2D cross section
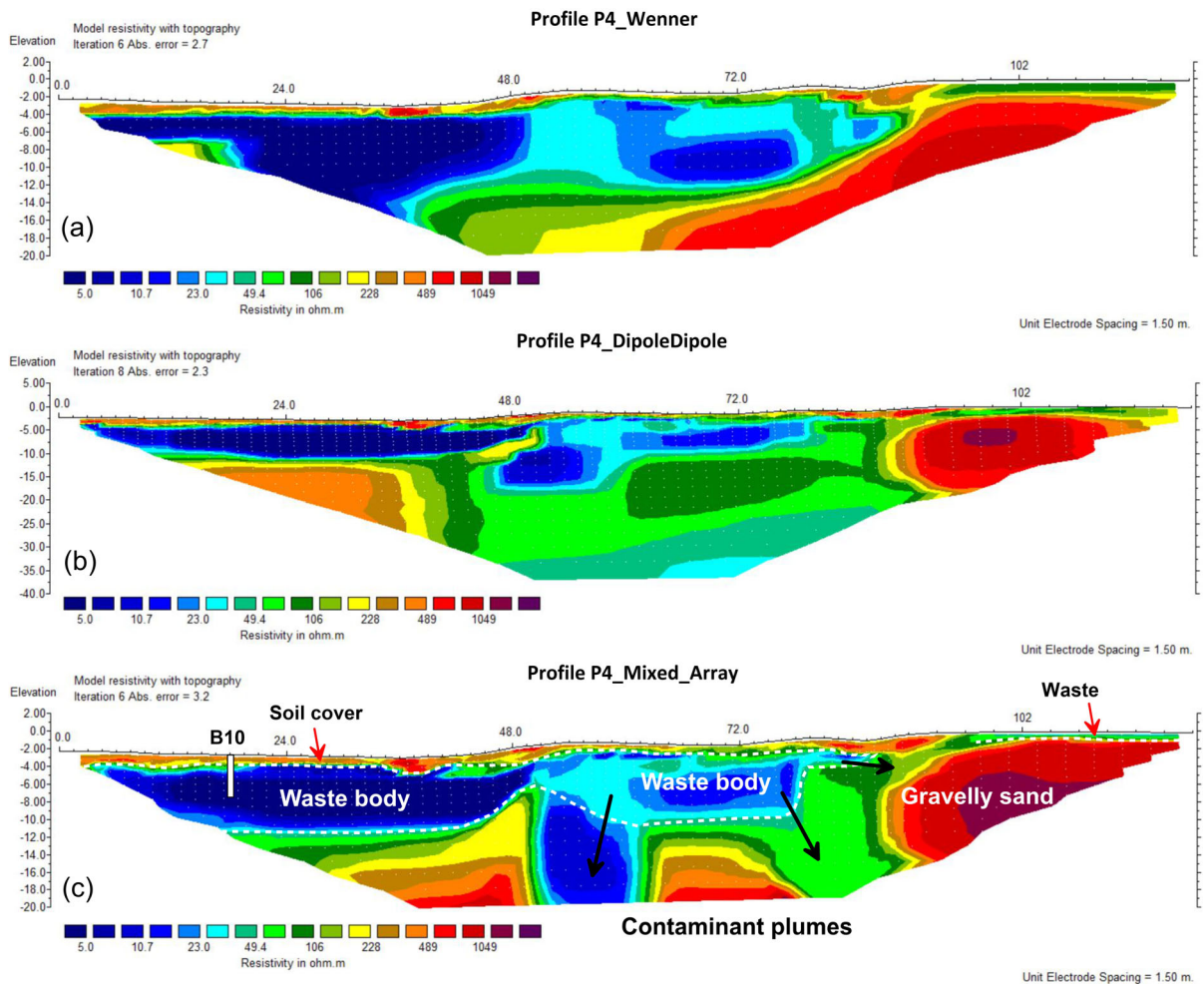
Figure 7
Inverted 2D resistivity model along ERT profile P4 obtained by Wenner array (**a**), dipole–dipole array (**b**), and mixed array (**c**). Black arrows refer to the possible pathways of leachate migration. Depth to the base of the landfill obtained from borehole B10 has been presented

resistivity zone with a thickness increasing from the south-eastern parts (about 5 m at profile P3) towards the north-western parts of the landfill (up to 15 m at profile P6). Leachate plumes originating from the landfill with low resistivities can be seen. They cause a huge decrease in the resistivity values of the gravelly sand layer. The results are in coincidence with the depths obtained from boreholes B2, B6 and B2. The correlation between the results of ERT data along profile P1 and the lithology of well W2 shows a good agreement. The resistivity values of the gravely sand layer obviously decrease below the groundwater table. Figure 10 presents the inverted model along the

ERT profiles P7 and P8. The measured apparent resistivity data of profile P7 showed large resistivity variations near the ground surface; therefore, a cell size of half the unit of the electrode spacing was utilized. This gives significantly better results (Loke, 2020). The Res2DInv software uses a model with a cell width equals to the unit of the electrode spacing by default. Also, to significantly decrease the inversion time which is a result of the increase of the cells from 1014 to 2653, the incomplete Gauss–Newton method was used to solve the least-squares equation. However, the standard (complete) Gauss–Newton method was used for the other profiles. Profile P7

Table 2

Overview of inversion parameters of the measured ERT profiles using the Res2DInv software

Profile	Type of array	Number of					Abs. error %	No. of electrodes	Length/ electrode spacing (m)
		Datum points	Data levels	Layers	Blocks	Iterations			
P1	Wenner	345	14	14	617	9	1.43	61	240/3
	Dipole–dipole	1072	43	21	1001	9	2.4		
	Mixed array	1363	50	17	826	9	4		
P2	Wenner	669	14	14	1177	7	2.9	101	300/2.5
	Dipole–dipole	2067	44	22	1896	9	4.4		
	Mixed array	2557	50	17	1509	9	3.2		
P3	Wenner	345	14	14	617	7	1.38	61	200/2.5
	Dipole–dipole	1048	44	22	1023	7	135		
	Mixed array	1342	50	17	832	8	1.4		
P4	Wenner	394	14	14	675	6	2.7	71	120/1.5
	Dipole–dipole	1309	46	23	1161	8	2.3		
	Mixed array	1595	50	17	931	6	3.2		
P5	Wenner	345	14	14	617	8	1.8	61	240/3
	Dipole–dipole	1059	43	21	1015	7	3.5		
	Schlumberger	745	25	18	827	8	1.8		
	Mixed array	1963	71	18	850	8	2.4		
P6	Wenner	343	14	14	615	7	2.5	61	240/3
	Dipole–dipole	1066	42	21	1001	7	4.8		
	Mixed array	1350	50	18	1716	8	3.8		
P7	Wenner	335	13	14	574	8	3.5	66	175/2.5
	Dipole–dipole	1014	42	27	2653	10	8.3		
	Mixed array	1349	49	23	2227	9	7.7		
P8	Wenner	345	14	14	615	8	1.6	61	60/0.75
	Dipole–dipole	1140	53	23	1039	9	5		
	Mixed array	1380	66	17	833	9	3.9		

extends 175 m parallel across the middle of the waste site. Its 2D ERT model depicts a clear distinction between three layers: the top soil cover (up to 3 m), the waste body and its leachate, and the bottom gravelly sand layer. It also shows that the waste body increases north-westwards (it exceeds 15 m at the start of the profile) and that it is not continuous but is interrupted at the distances 41 m and 125 m, which divides the area into three portions. This result coincides with the findings obtained by the magnetic survey. Borehole B3 shows that the depth to the base of the landfill at the center of this profile (at distance 97 m) is 7.8 m which is less than the depth (about 11 m) inferred from the ERT data reflecting a leachate infiltration. The ERT profile P8 was chosen to cut an interesting U-shaped highly magnetic anomaly (refer to Fig. 4). The profile extends to 60 m using 61 electrodes with an electrode spacing of 0.75 m. This U-shaped highly magnetic structure coincides with a very conductive body (0.3–15 Ω m), which refers to an accumulation of metallic materials in this part of

the study area. The waste body is separated with a resistive division between the distances 13 m and 15 m. The cover soil has a thickness range of 0.5–2 m.

To examine the proficiency of the ERT method in imaging the landfill geometry, a synthetic ERT model (Fig. 11a) was constructed using the Res2Dmod software (Loke, 2016) based on the available geological information as well as on the obtained resistivity values of the waste body and its surrounding layers (refer to Fig. 6) in the present research. The finite-difference method was used in the resistivity forward modelling to calculate the apparent resistivity values. The model consists of a 3 m topmost soil layer with a resistivity value of 250 Ω m, a gravelly sand layer with a resistivity of 1000 Ω m and a thickness of 17 m, a base layer with a resistivity of 50 Ω m, and finally a low resistivity layer (10 Ω m) within the gravelly sand layer representing the waste materials of the landfill. The apparent resistivity pseudosection for the constructed model was calculated (Fig. 11b). Sixty-one electrodes
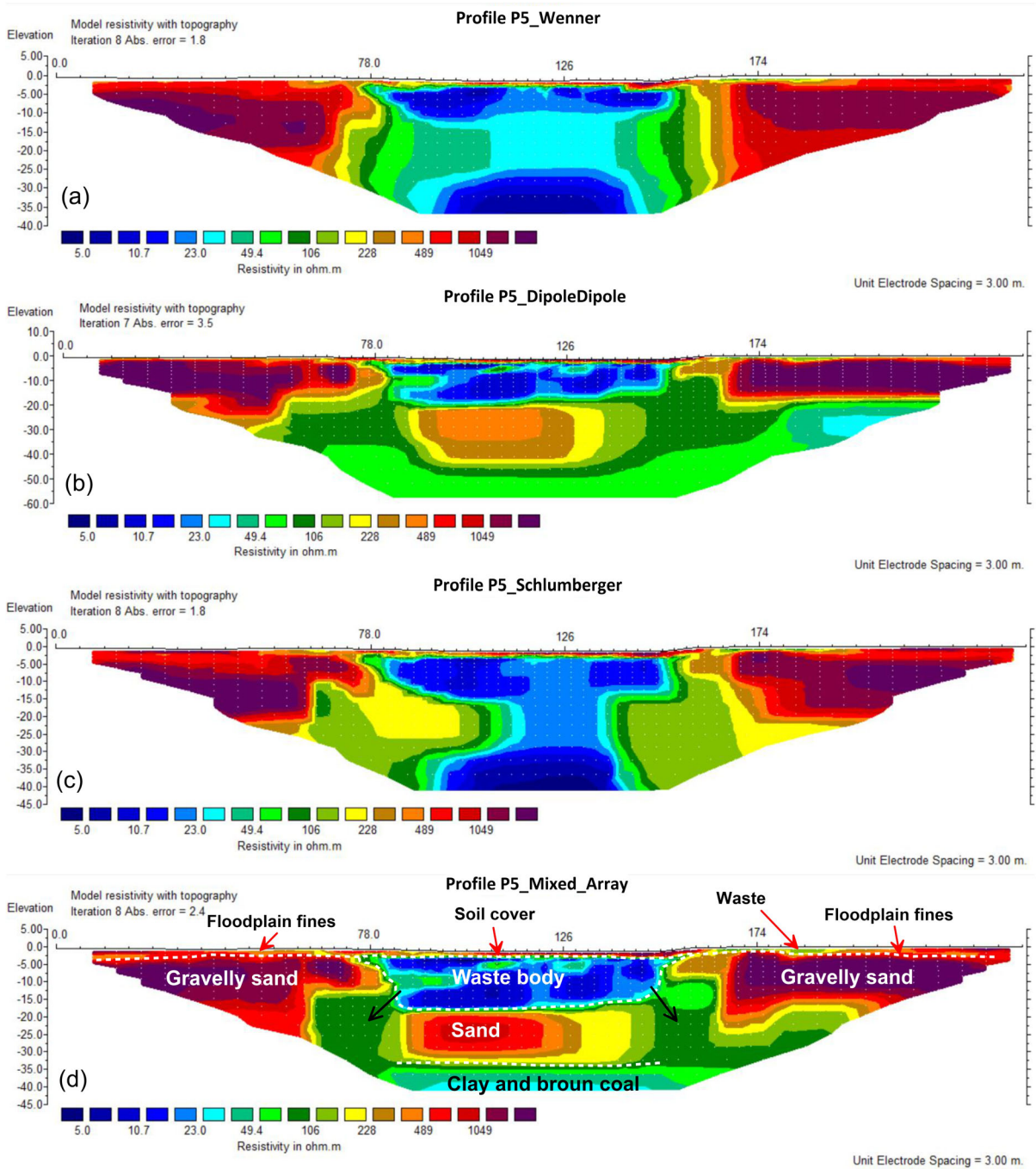
Figure 8
Inverted 2D resistivity model along ERT profile P5 obtained by Wenner array (**a**), dipole–dipole array (**b**), Schlumberger array (**c**), and mixed array (**d**). Black arrows refer to the possible pathways of leachate migration

and an electrode spacing of 3 m were used to form an ERT profile extending along a distance of 180 m. The

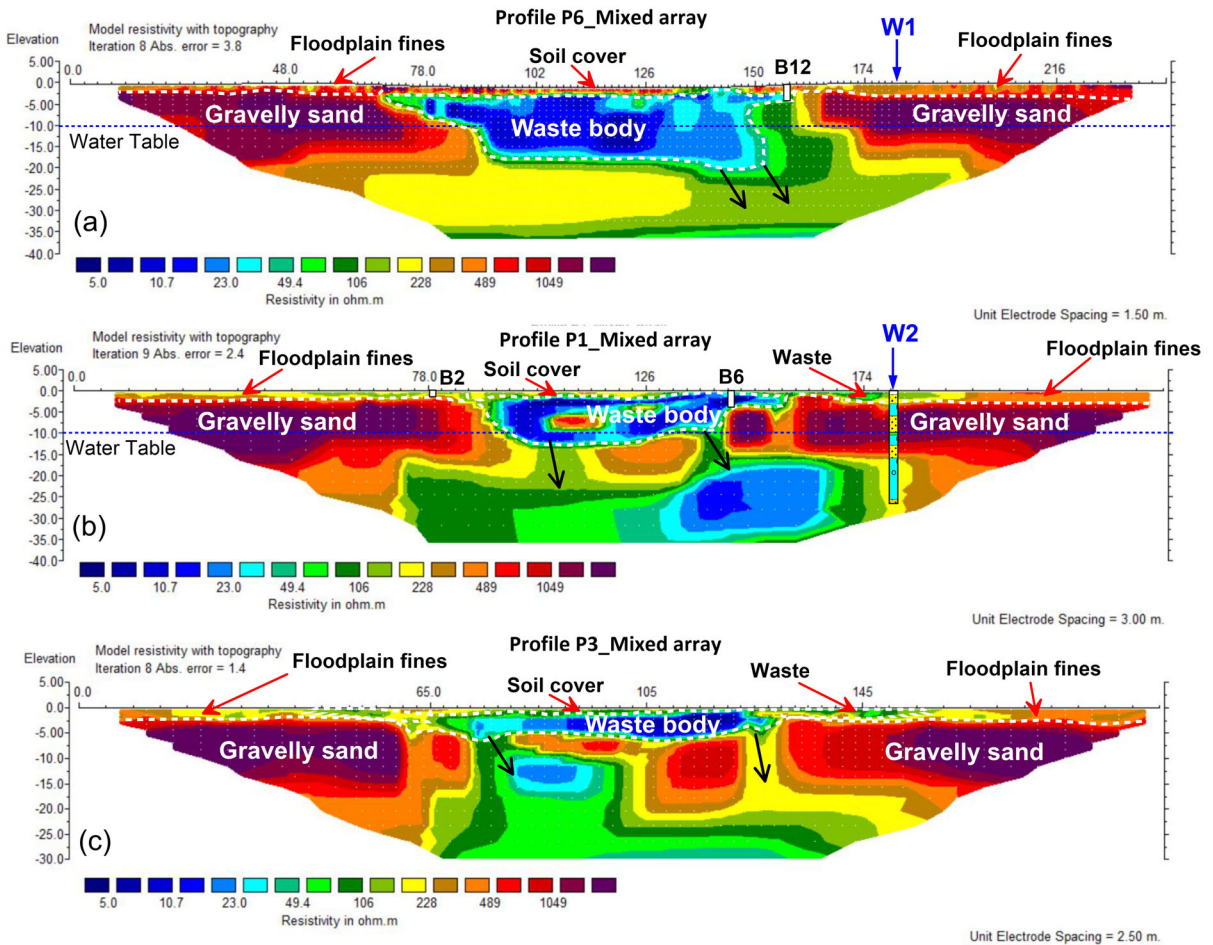inversion of the obtained data was carried out using the robust technique. The results (Fig. 11) show that

Figure 9

The inversion 2D models produced by the robust (L1-norm) inversion method using mixed array for the ERT profiles P6 (**a**), P1 (**b**), and P3 (**c**). Black arrows refer to the possible pathways of leachate migration. Locations and depths of boreholes B2 (8 m to the northwest of profile P1), B6 (13 m to the south of profile P1), and B12 (5 m to the north of profile P6) as well as the locations of observation wells W1 and W2 in addition to the lithology of well W2 are presented (yellow colour refers to sand and turquoise represents the gravel). The groundwater table is recorded at depth of 10 m

the geometry of the landfill was successfully resolved with sharp boundaries and a good Absolute error (2.1%). Another similar synthetic model was created, but a low resistivity zone (25 Ω m) representing the pathway of a leachate plume was added as shown in Fig. 12. The inverted resistivity section of this model shows the efficiency of the ERT method in imaging the migration pathways of the pollutants from the dumping site. This synthetic study supports our ERT results.

The 3D subsurface image of the landfill generated by combining inverted ERT data from all profiles is presented in Fig. 13. The 3D subsurface resistivity

model presents the distribution of resistivity values ranging between less than 5 Ω m and several thousands of Ω m. In general, high resistivity values are corresponding to the capping soil and the gravelly sand layer, and very low resistivities to the waste body, its leachates, and contamination plumes. A thin layer of dry waste materials with a thickness of up to 2 m and resistivity values of 50–100 Ω m extending outside the main mass of the waste body towards the East can be clearly seen on profiles P1–P5 (refer to Fig. 13). This 3D perspective shows possible leakage pathways of contaminates along low resistivity zone at the boundaries of the landfill towards deeper
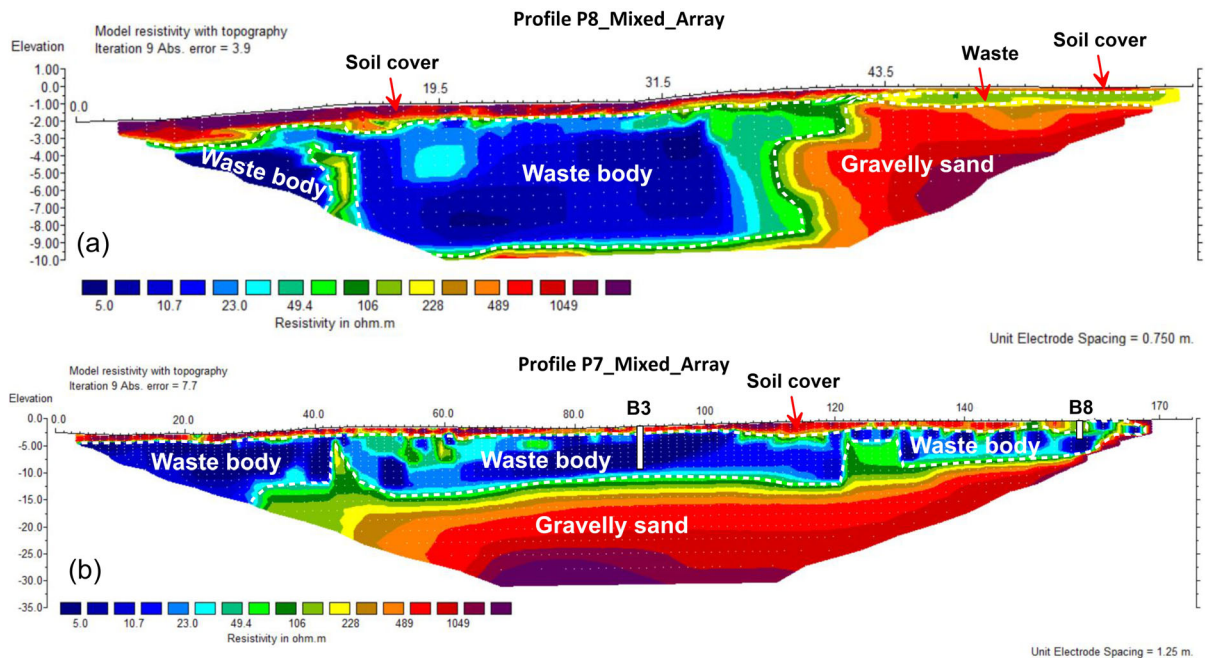
Figure 10
Inverted 2D resistivity models produced by the robust (L1-norm) inversion method using mixed array for the ERT profiles P8 (**a**) and P7 (**b**). Location and depth to the base of landfill obtained from boreholes B3 and B8 (5 m to the west of profile P7) are presented on the inverted 2D ERT model of profile P7

layers. Generally, the depth to the base of the waste body increases towards the north-west. Moreover, the boundaries of the landfill are evidently distinguished from the hosting medium. We also noticed that the leakage of contaminants occurred at the boundaries of the landfill, particularly at its eastern parts (see also Figs. 6, 8d and 9) which is in agreement with the flow direction of the groundwater in the area. By comparing the ERT results with the magnetic maps, it is noticed that the low resistivity anomalies correspond with highly magnetic anomalies in many localities. This confirms the presence of the metal content.

5. Conclusions

In the present study, we were able to successfully determine the geometry of a landfill located to the north-west of Cologne, Germany by using the integration of magnetic and ERT geophysical techniques. Both techniques show that the landfill distributes on

an area of about 19,000 m². It has a length of more than 190 m and an average width of approximately 100 m. We also differentiated between places where magnetic and non-magnetic materials were dumped. Lots of subsurface magnetic bodies were observed within the undisturbed geology outside the landfill site which can be interpreted as discarded iron materials or could resemble UXOs, explosive remnants of World War II which must be taken into account. Gas pipelines that run to the south of the area were perfectly imaged by the magnetic survey. A significant consistency between the two methods in determining the horizontal edges of the waste site was observed. The results show that the waste body has very low resistivities compared with the highly resistive hosting gravelly sand layer, which facilitates imaging the landfill. Low resistivity signatures at depths deeper than those expected indicate an infiltration of contaminant leachates downwards through the base of the saturated landfill. These potential migration pathways of leachate plumes were delineated quite distinctly.
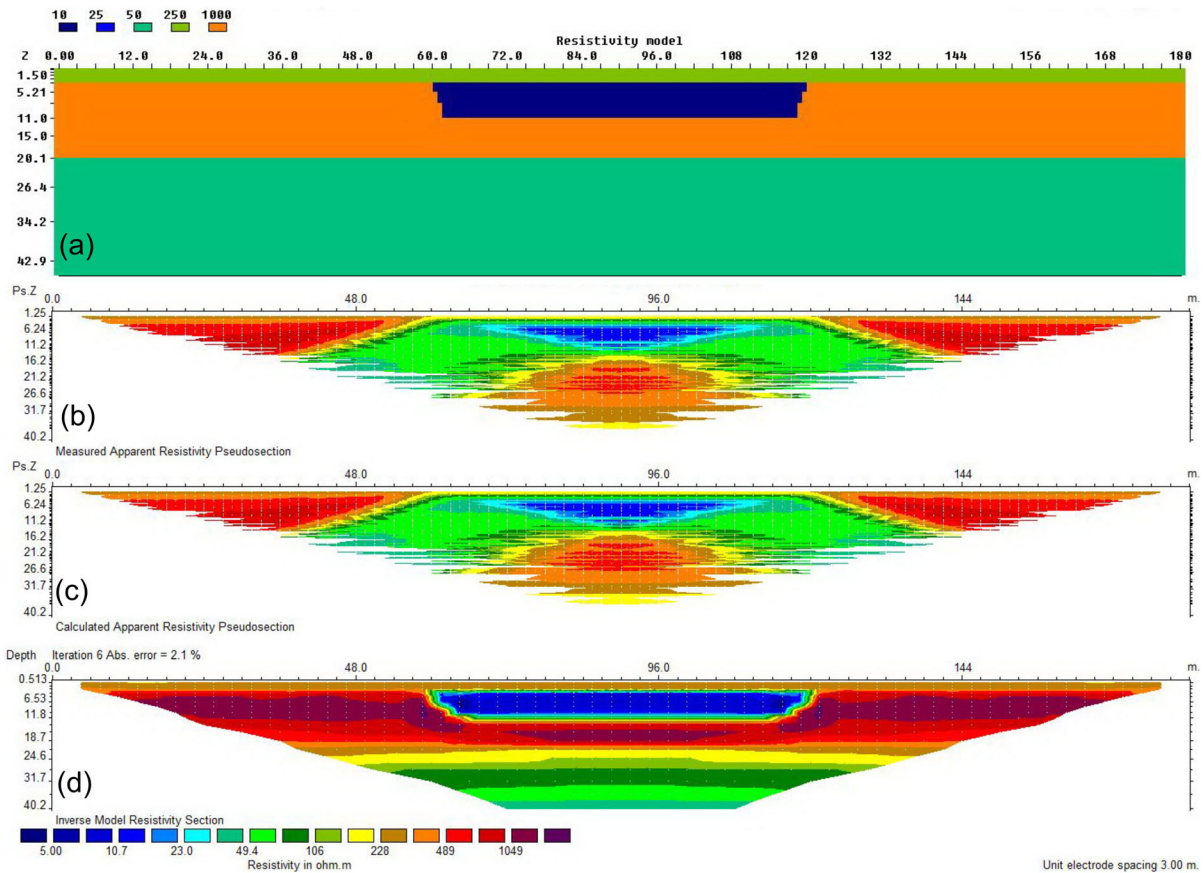
Figure 11

a Synthetic 2D model representing the landfill site, **b** measured apparent resistivity pseudosection, **c** calculated apparent resistivity pseudosection, and **d** the inverted 2D resistivity model using robust inversion of the obtained ERT data after 6 iterations (absolute error = 2.1%)

Though the mixed array significantly increases the time and cost of the ERT survey, it can be considered as the best configuration for imaging the landfill alongside the other three standard arrays (Wenner, dipole–dipole, and Schlumberger). The Wenner and Schlumberger arrays could not detect the base of the landfill; therefore, one should avoid them in studies dealing with landfill characterization. However, the dipole–dipole array gave reasonable results hence it can be recommended as a second option after the mixed array. Moreover, the robust (L1-norm) inversion method produced more accurate resistivity models with sharp boundaries between the layers than the smoothness-constrained least-squares (L2-norm) method due to the high contrasts in electrical resistivity values between the dumped waste and the host

medium. Therefore, we strongly recommend it for landfill studies.

The findings of this study exhibit the efficiency of using a combination of geophysical methods for the characterization of landfills. They also shed the light on the serious environmental problem of groundwater contamination in the study area. A properly treatment of the landfill leachate in the surveyed area and determining an appropriate remedial action is essential and highly recommended.
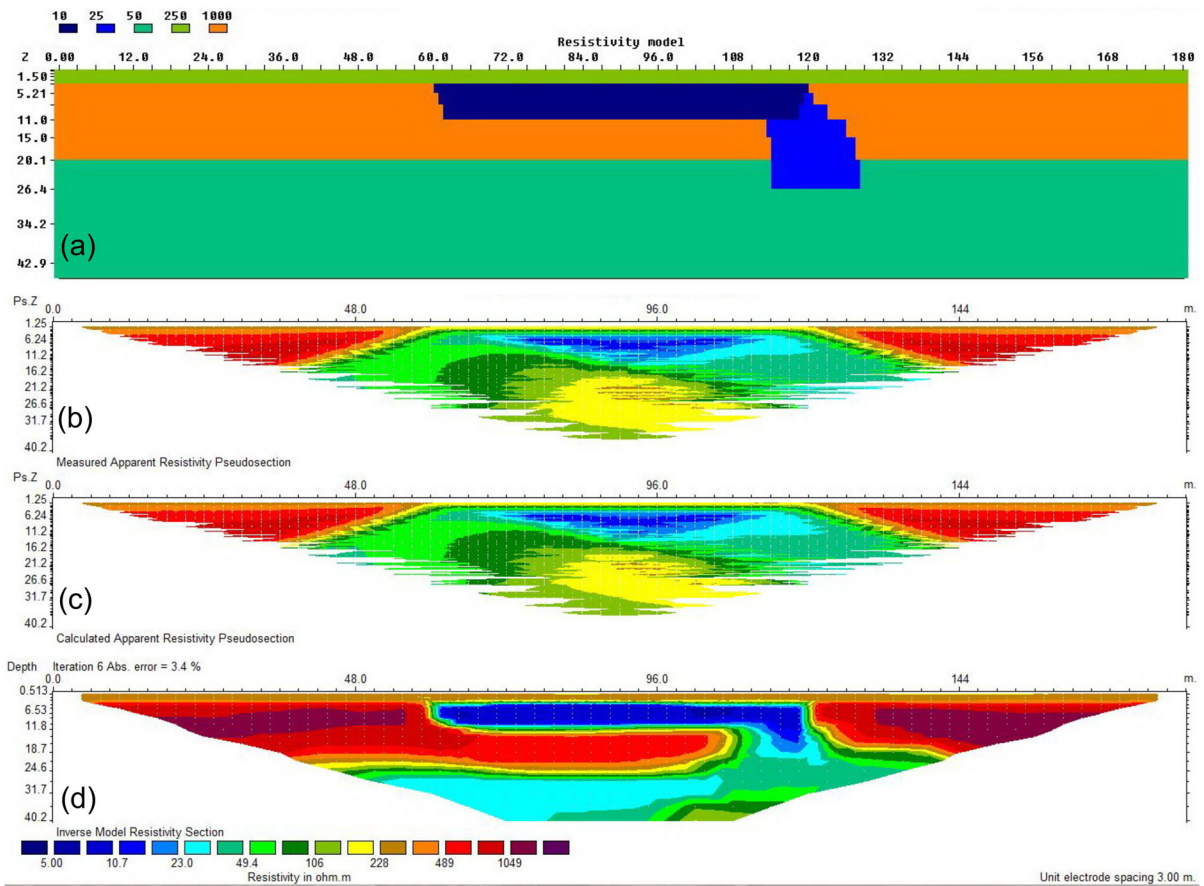
Acknowledgements

Figure 12
a Synthetic 2D model representing the landfill site and a pathway of a leachate plume, b measured apparent resistivity pseudosection, c calculated apparent resistivity pseudosection, and d the inverted 2D resistivity model using robust inversion of the obtained ERT data after 6 iterations (absolute error = 3.4%)
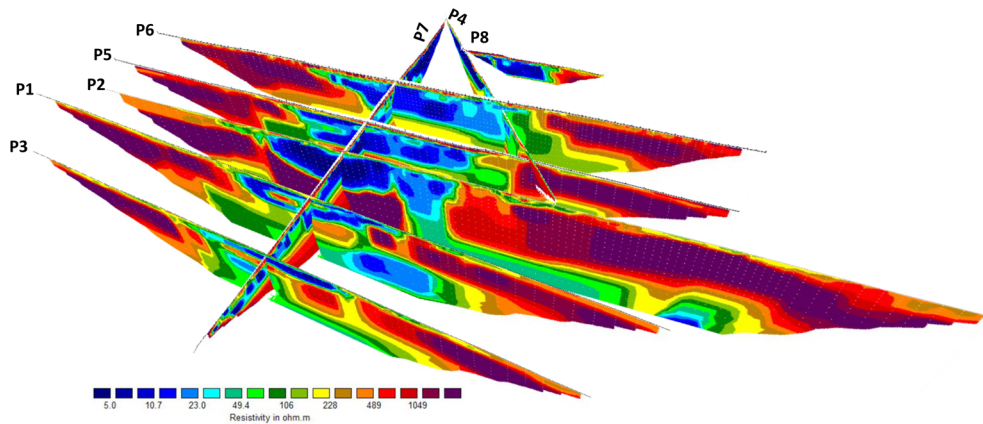

Figure 13
3D subsurface resistivity distribution in the landfill area and its surroundings. The lateral and vertical extensions of the waste body have been clearly imaged. Contamination plumes can be seen at the eastern boundary of the landfill which is in agreement with the groundwater flow in the area

Az: 94911/2018). We would also like to sincerely thank the environmental department of the City of Cologne for granting permission to access the landfill site and providing us with borehole logs and geological information. The cooperation of K.M. Gerhold from the City of Cologne is greatly acknowledged. We thank the Editor and the three anonymous reviewers for their great efforts and valuable constructive comments, which helped us to improve our manuscript.

Code availability

Not applicable.

Declarations

Conflict of interest The authors have no conflicts of interest to declare that are relevant to the content of this article.

Availability of data and material (data transparency) The authors confirm that all data and materials as well as software application support their published claims and comply with field standards. The data that support the findings of this study are available from the corresponding author upon reasonable request.

Publisher's Note Springer Nature remains neutral with regard to jurisdictional claims in published maps and institutional affiliations.

REFERENCES

Appiah, I., Wemegah, D. D., Asare, V.-D.S., Danuor, S. K., & Forson, E. D. (2018). Integrated geophysical characterisation of Sunyani municipal solid waste disposal site using magnetic gradiometry, magnetic susceptibility survey and electrical resistivity tomography. *Journal of Applied Geophysics, 153*, 143–153. https://doi.org/10.1016/j.jappgeo.2018.02.007

Arisoy, M., & Dikmen, Ü. (2013). Edge detection of magnetic sources using enhanced total horizontal derivative of the Tilt angle. *Bulletin of the Earth Sciences Application and Research Centre of Hacettepe University, 34*(1), 73–82

Baawain, M. S., Al-Futaisi, A. M., Ebrahimi, A., & Omidvarborna, H. (2018). Characterizing leachate contamination in a landfill site using TDEM (time domain electromagnetic) imaging. *Journal of Applied Geophysics, 151*, 73–81. https://doi.org/10.1016/j.jappgeo.2018.02.002

Bernstone, C., & Dahlin, T. (1997). DC resistivity mapping of old landfills: Two case studies. *European Journal of Environmental Engineering Geophysics, 2*, 121–136

Candansayar, M. E., & Tezkan, B. (2006). A comparison of different radiomagnetotelluric data inversion methods for buried waste sites. *Journal of Applied Geophysics, 58*(3), 218–231. https://doi.org/10.1016/j.jappgeo.2005.07.001

Cardarelli, E., & De Donno, G. (2019). Advances in electric resistivity tomography: Theory and case studies. In R. Persico, S. Piro, & N. Linford (Eds.), *Innovation in near-surface geophysics.* (pp. 23–57). Elsevier.

Carpenter, P. J., Calkin, S. F., & Kaufmann, R. S. (1991). Assessing a fractured landfill cover using electrical resistivity and seismic refraction techniques. *Geophysics, 56*(11), 1896–1904. https://doi.org/10.1190/1.1443001

Claerbout, J. F., & Muir, F. (1973). Robust modeling with erratic data. *Geophysics, 38*, 826–844

Dahlin, T., & Zhou, B. (2004). A numerical comparison of 2D resistivity imaging with 10 electrode arrays. *Geophysical Prospecting, 52*, 379–398

De Carlo, L., Perri, M. T., Caputo, M. C., Deiana, R., Vurro, M., & Cassiani, G. (2013). Characterization of a dismissed landfill via electrical resistivity tomography and mise-à-la-masse method. *Journal of Applied Geophysics, 98*, 1–10. https://doi.org/10.1016/j.jappgeo.2013.07.010

De Iaco, R., Green, A. G., Maurer, H.-R., & Horstmeyer, H. (2003). A combined seismic reflection and refraction study of a landfill and its host sediments. *Journal of Applied Geophysics, 52*(4), 139–156. https://doi.org/10.1016/s0926-9851(02)00255-0

Dumont, G., Robert, T., Mark, N., & Nguyen, F. (2017). Assessment of multiple geophysical techniques for the characterization of municipal waste deposit sites. *Journal of Applied Geophysics, 145*, 74–83

Frangos, W. (1997). Electrical detection of leaks in lined waste disposal ponds. *Geophysics, 62*(6), 1737–1744. https://doi.org/10.1190/1.1444274

Genelle, F., Sirieix, C., Riss, J., Naudet, V., Dabas, M., & Bégassat, P. (2014). Detection of landfill cover damage using geophysical methods. *Near Surface Geophysics, 12*, 599–611

Helene, L. P. I., Moreira, C. A., & Bovi, R. C. (2020). Identification of leachate infiltration and its flow pathway in landfill by means of electrical resistivity tomography (ERT). *Environmental Monitoring and Assessment*. https://doi.org/10.1007/s10661-020-8206-5

Heuser, H., & Thielmann, G. (1986). *Ingenieurgeologische Karten 1:25000/Köln map*. (1st ed.). Geologischer Dienst Nordrhein. In German.

Hinze, W. J., von Frese, R. R. B., & Saad, A. H. (2013). *Gravity and magnetic exploration: Principles, practices, and applications*. (p. 282). Cambridge University Press.

Ibraheem, I. M., Elawadi, E. A., & El-Qady, G. M. (2018a). Structural interpretation of aeromagnetic data for the Wadi El Natrun area, Northwestern Desert, Egypt. *Journal of African Earth Sciences, 139*, 14–25

Ibraheem, I. M., Gurk, M., Tougiannidis, N., & Tezkan, B. (2018b). Subsurface imaging of the Neogene Mygdonian basin, Greece using magnetic data. *Pure and Applied Geophysics, 175*(8), 2955–2973

Ibraheem, I. M., Haggag, M., & Tezkan, B. (2019). Edge detectors as structural imaging tools using aeromagnetic data: A case study of Sohag Area, Egypt. *Geosciences, 9*(5), 211

Isles, D. J., & Rankin, L. R. (2013). *Geological interpretation of aeromagnetic data*. (p. 365). CSIRO publishing.

Jeng, Y., Lee, Y. L., Chen, C. Y., & Lin, M. J. (2003). Integrated signal enhancements in magnetic investigation in archaeology. *Journal of Applied Geophysics, 53*, 31–48

Karlık, G., & Kaya, M. A. (2001). Investigation of groundwater contamination using electric and electromagnetic methods at an open waste-disposal site: A case study from Isparta, Turkey. *Environmental Geology, 40*(6), 725–731. https://doi.org/10.1007/s002540000232

Kaufmann, O., & Quinif, Y. (2001). An application of cone penetration tests and combined array 2D electrical resistivity to delineate cover-collapse sinkhole prone areas. In B. F. Beck & J. G. Herring (Eds.), *Geotechnical and environmental applications of karst geology and hydrology.* (pp. 359–364). Balkema.

Kirsch, R. (2009). Groundwater protection: mapping of contaminations. In R. Kirsch (Ed.), *Groundwater geophysics—a tool for hydrogeology.* (2nd ed., pp. 525–539). Springer.

Leucci, G. (2020). *Advances in geophysical methods applied to forensic investigations new developments in acquisition and data analysis methodologies*. Springer. https://doi.org/10.1007/978-3-030-46242-0

Li, X. (2006). Understanding 3D analytic signal amplitude. *Geophysics, 71*(2), L13–L16. https://doi.org/10.1190/1.2184367

Loke, M. H. (2016). RES2DMOD ver. 3.03: Rapid 2D resistivity and I.P. forward modeling using the finite-difference and finite-element methods, Geotomo Software, Malaysia, p. 25.

Loke, M. H. (2020). Tutorial: 2-D and 3-D electrical imaging surveys. Geotomosoft Solutions, Malaysia. www.geotomosoft.com. Accessed 18 Mar 2020.

Loke, M. H., Acworth, I., & Dahlin, T. (2003). A comparison of smooth and blocky inversion methods in 2D electrical imaging surveys. *Exploration Geophysics, 34*, 182–187

Marchetti, M., Cafarella, L., Di Mauro, D., & Zirizzotti, A. (2002). Ground magnetometric surveys and integrated geophysical methods for solid buried waste detection: a case study. *Annals of Geophysics, 45*(3/4), 563–573

Martinho, E., & Almeida, F. (2006). 3D behaviour of contamination in landfill sites using 2D resistivity/IP imaging: Case studies in Portugal. *Environmental Geology, 49*(7), 1071–1078. https://doi.org/10.1007/s00254-005-0151-7

Mepaiyeda, S., Madi, K., Gwavava, O., Baiyegunhi, C., & Sigabi, L. (2019). Contaminant delineation of a landfill site using electrical resistivity and induced polarization methods in Alice, Eastern Cape, South Africa. *International Journal of Geophysics*. https://doi.org/10.1155/2019/5057832

Missiaen, T., & Feller, P. (2008). Very-high-resolution seismic and magnetic investigations of a chemical munition dumpsite in the Baltic Sea. *Journal of Applied Geophysics, 65*(3–4), 142–154. https://doi.org/10.1016/j.jappgeo.2008.07.001

Morita, A. K. M., de Souza Pelinson, N., Elis, V. R., & Wendland, E. (2020). Long-term geophysical monitoring of an abandoned dumpsite area in a Guarani Aquifer recharge zone. *Journal of Contaminant Hydrology*. https://doi.org/10.1016/j.jconhyd.2020.103623

Ogilvy, R., Meldrum, P., Chambers, J., & Williams, G. (2002). The use of 3D electrical resistivity tomography to characterise waste and leachate distribution within a closed landfill, Thriplow, UK. *Journal of Environmental and Engineering Geophysics, 7*(1), 11–18. https://doi.org/10.4133/JEEG7.1.11

Orlando, L., & Marchesi, E. (2001). Georadar as a tool to identify and characterise solid waste dump deposits. *Journal of Applied Geophysics, 48*(3), 163–174. https://doi.org/10.1016/s0926-9851(01)00088-x

Porsani, J. L., Filho, W. M., Elis, V. R., Shimeles, F., Dourado, J. C., & Moura, H. P. (2004). The use of GPR and VES in delineating a contamination plume in a landfill site: A case study in SE Brazil. *Journal of Applied Geophysics, 55*(3–4), 199–209. https://doi.org/10.1016/j.jappgeo.2003.11.001

Prezzi, C., Orgeira, M. J., Ostera, H., & Vásquez, C. A. (2005). Ground magnetic survey of a municipal solid waste landfill: Pilot study in Argentina. *Environmental Geology, 47*(7), 889–897. https://doi.org/10.1007/s00254-004-1198-6

Ramalho, E. C., Dill, A. C., & Rocha, R. (2013). Assessment of the leachate movement in a sealed landfill using geophysical methods. *Environmental Earth Sciences, 68*(2), 343–354. https://doi.org/10.1007/s12665-012-1742-8

Reynolds, J. M. (2011). *An introduction to applied and environmental geophysics*. (2nd ed.). Wiley.

Roest, W. R., Verhoef, J., & Pilkington, M. (1992). Magnetic interpretation using the 3-D analytic signal. *Geophysics, 57*(1), 116–125

Saraev, A., Simakov, A., Tezkan, B., Tokarev, I., & Shlykov, A. (2020). On the study of industrial waste sites on the Karelian Isthmus/Russia using the RMT and CSRMT methods. *Journal of Applied Geophysics, 175*, 103993. https://doi.org/10.1016/j.jappgeo.2020.103993

Sharma, P. V. (1997). *Environmental and engineering geophysics*. (pp. 78–79). Cambridge University Press.

Simyrdanis, K., Papadopoulos, N., Soupios, P., Kirkou, S., & Tsourlos, P. (2018). Characterization and monitoring of subsurface contamination from Olive Oil Mills' waste waters using Electrical Resistivity Tomography. *Science of the Total Environment, 637–638*, 991–1003. https://doi.org/10.1016/j.scitotenv.2018.04.348

Song, S.-H., Cho, I.-K., Lee, G.-S., Yong, H.-H., & Um, J.-Y. (2019). Delineation of leachate pathways using electrical methods: Case history on a waste plaster landfill in South Korea. *Exploration Geophysics, 51*(3), 301–313

Soupios, P., & Ntarlagiannis, D. (2017). Characterization and monitoring of solid waste disposal sites using geophysical methods: Current applications and novel trends. In D. Sengupta & S. Agrahari (Eds.), *Modelling trends in solid and hazardous waste management.* (pp. 75–103). Springer.

Telford, W. M., Geldart, L. P., Sheriff, R. E., & Keys, D. A. (1990). *Applied geophysics.* (2nd ed.). Cambridge University Press.

Tezkan, B. (1999). A review of environmental applications of quasi-stationary electromagnetic techniques. *Surveys in Geophysics, 20,* 279–308

Tezkan, B., Goldman, M., Greinwald, S., Hördt, A., Müller, I., Neubauer, F. M., & Zacher, G. (1996). A joint application of radiomagnetotellurics and transient electromagnetics to the investigation of a waste deposit in Cologne (Germany). *Journal of Applied Geophysics, 34,* 199–212. https://doi.org/10.1016/0926-9851(95)00016-X

Tezkan, B., Hördt, A., & Gobashy, M. (2000). Two-dimensional radiomagnetotelluric investigation of industrial and domestic waste sites in Germany. *Journal of Applied Geophysics, 44*(2–3), 237–256. https://doi.org/10.1016/s0926-9851(99)00014-2

Wemegah, D. D., Fiandaca, G., Auken, E., Menyeh, A., & Danour, S. K. (2017). Spectral time-domain induced polarization and magnetics surveying—an efficient tool for characterisation of solid waste deposits in developing countries. *Near Surface Geophysics, 15*(1), 75–84

Wolke, R., & Schwetlick, H. (1988). Iteratively reweighted least-squares algorithms, convergence analysis, and numerical comparisons. *SIAM Journal of Scientific and Statistical Computations, 9,* 907–921

Wu, T.-N., & Huang, Y.-C. (2006). Detection of illegal dump deposit with GPR: Case study. *Practice Periodical of Hazardous, Toxic, and Radioactive Waste Management, 10*(3), 144–149. https://doi.org/10.1061/(asce)1090-025x(2006)10,3(144)

Yannah, M., Martens, K., Van Camp, M., & Walraevens, K. (2019). Geophysical exploration of an old dumpsite in the perspective of enhanced landfill mining in Kermt area, Belgium. *Bulletin of Engineering Geology and the Environment, 78,* 55–67. https://doi.org/10.1007/s10064-017-1169-2

Zhou, B., & Dahlin, T. (2003). Properties and effects of measurement errors on 2D resistivity imaging surveying. *Near Surface Geophysics, 1,* 105–117

Zhou, W., Beck, B., & Adams, A. (2002). Effective electrode array in mapping karst hazards in electrical resistivity tomography. *Environmental Geology, 42*(8), 922–928. https://doi.org/10.1007/s00254-002-0594-z